CNC/AgNP hybrids as safer-by-design biocides in paints

Dafné Musino, Aurélie Rosset, Cécile Lelong, Sylvie Luche, Virginie Bergé, Grégory Brochard, Manon Plumail, Bénédicte Trouiller, Aurélien Auger, Arnaud Guiot, et al.

▶ **To cite this version:**

Dafné Musino, Aurélie Rosset, Cécile Lelong, Sylvie Luche, Virginie Bergé, et al.. CNC/AgNP hybrids as safer-by-design biocides in paints. Environmental science.Nano, 2021, 8 (12), pp.3673-3684. 10.1039/d1en00407g . hal-03417304

HAL Id: hal-03417304
https://hal.science/hal-03417304

Submitted on 4 Jan 2022

HAL is a multi-disciplinary open access archive for the deposit and dissemination of scientific research documents, whether they are published or not. The documents may come from teaching and research institutions in France or abroad, or from public or private research centers.

L'archive ouverte pluridisciplinaire **HAL**, est destinée au dépôt et à la diffusion de documents scientifiques de niveau recherche, publiés ou non, émanant des établissements d'enseignement et de recherche français ou étrangers, des laboratoires publics ou privés.

This document is the post-print version of the article originally published in Environmental Science Nano 2021, 8 (12), pp.3673-3684 under the doi: 10.1039/D1EN00407G

CNC/AgNP hybrids as safer-by-design biocides in paints

Dafne Musino,[a] Aurélie Rosset,[b] Cécile Lelong,[c] Sylvie Luche,[c] Virginie Bergé,[d] Grégory Brochard,[d] Manon Plumail,[e] Benedicte Trouiller,[e] Aurélien Auger,[f] Arnaud Guiot,[b] Julien Patouillard,[b] Stephanie Desrousseaux[b], Sébastien Artous,[b] Thierry Rabilloud,[c] Delphine Boutry, [b] Isabelle Capron [a]

[a] *INRAE, BIA, 44316, Nantes, France*

[b] *Univ. Grenoble Alpes, CEA, LITEN, DTNM, LMSE, F-38000 Grenoble, France*

[c] *Univ. Grenoble Alpes, CNRS, CEA, IRIG, CBM, Laboratoire de Chimie et Biologie des Métaux, UMR5249, 38000 Grenoble, France*

[d] *ALLIOS, Les Docks Mogador, 13011 Marseille, France*

[e] *INERIS, Parc Alata, BP2, 60550 Vernueil-en-Halatte, France*

[f] Univ. Grenoble Alpes, CEA, LITEN, DTNM, LVME, F-38000 Grenoble, France

ABSTRACT

In this work, a biocidal paints is designed by a safer-by-design approach where an efficient antibacterial activity is provided by nanohybrids consisting in silver nanoparticles (AgNPs) nucleated on a bio-based substrate (cellulose nanocrystals, CNCs), to be included in an amount as low as possible and dispersed in aqueous suspension. Three CNC/AgNP hybrids varying in CNC surface modifications are characterized in depth by transmission electron microscopy, atomic absorption spectroscopy and X-ray diffraction, and used in realistic paint formulations. The analysis of dry-films degradation followed by artificial weathering and mechanical solicitation (i.e., abrasion) reveals a reduced airborne emission of particles that could have harmful impact on human health and environment. However life cycle assessment shows a weak beneficial impact due to the low amount compared to paint manufacturing impact. Finally, the biocidal activity was clearly detected on dry paints using *Bacillus Subtilis* bacterium. It demonstrates that the resulting dry-state paints containing the AgNPs best dispersed and with the smallest size (i.e., 11 nm) show the strongest biocidal effect. This approach allows considerably reducing the Ag amount to reach an antibacterial effect comparable to AgCl. Moreover, no specific toxicity is revealed and only biodegradable CNCs will persist in environment at the end of the antimicrobial activity provided by AgNPs. The development of such

CNC/AgNP hybrids, considering the overall life cycle of the material like paint, opens the road to the development of highly efficient and more eco-friendly materials.

KEYWORDS. Biocidal paints, Silver nanoparticles (AgNPs), Cellulose nanocristals, Hybrids, Sustainable biocide, Artificial weathering. Risk assessment,

INTRODUCTION.

With the recent health crises, processing and building industry is showing great interest in paints and coating films with biocidal properties because of their capability to avoid or reduce microorganism growing.[1–4] Concerning interior-exterior paints, the biocidal activity is required to prevent the spoilage of the wet-state paint during storage since absence of biocide in paint formulation can lead to the formation of a biofilm on the paint surface, representing a technical issue and eventually a risk for human health.[5,6] Also, the addition of biocidal agents allows ensuring a long-term dry-film performance, preventing degradation phenomena such as discoloration and degradation.[7–9] Finally, paints and coatings with biocidal properties are not only more and more expected in medical environment such as hospital surface or doctor waiting rooms[8,10,11] but also in everyday life (e.g., house painting) in order to reduce infections due to presence of airborne or hand-deposited pathogenic microorganisms.[11] Hence, the formulation of paints with biocidal agents is consequently essential to preserve the paint characteristics in wet- and dry-state. Isothiazolinone-based biocides, such as methylisothiazolinone (MIT), chloromethylisothiazolinone (CMIT or CIT) or benzisothiazolinone (BIT), are widely used in coating and paint manufacturing because of their capability to penetrate the bacterial membrane and fungal cell walls blocking cell functions.[4,12,13] They are usually mixed together to ensure a long-term preservation and to obtain a broad-spectrum bactericide. However, it has been proved that most of these commercial biocides have potentially dangerous effects since they can cause cutaneous and respiratory allergy,[14,15] raising the question of toxicity for human health, and environmental impact in the paint formulation. The idea is to anticipate such hazardous effects following a "safer-by-design" approach[16] which consists in the conception of the material considering all its whole life cycle assessment to manage the environmental health security (EHS) and in the optimization of the benefit/risk ratio in terms of social and economic paths.[16]

In this context, silver nanoparticles (AgNPs) and silver-based compounds (e.g., hybrid nanoparticles or nanomaterials) represent a promising alternative to classic commercial biocides to obtain an efficient antimicrobial effect in coatings and paints because of their efficiency at low concentration and their easy incorporation during paint production. AgNPs are known for their antibacterial properties.[17] The AgNP biocidal activity is mainly governed by the oxidative dissolution of AgNPs and its interaction with the bacteria membrane[18], with performance enhanced by the NP high surface area per volume unit.[19] Bechtold at al.[2] assess the biocidal effect of AgNPs with an average diameter

of 40 nm dispersed in polyurethane based paints, indicating that the microorganism development was prevented by the presence of AgNPs at a concentration of 500 ppm, but that such an AgNP content is not enough to inhibit fungi growing. Kumar and co-workers[20] synthetized AgNP embedded paints based on vegetal oil which show excellent antimicrobial properties tested against Gram-positive human pathogens (*Staphylococcus aureus*) and Gram-negative bacteria (*Escherichia coli*). Furthermore, they indicate that Ag^+ ions have a low toxicity for human cells and that the NP form seems to be harmless for human health.[2,6,20–23] However, additional studies are strongly encouraged in the field of AgNP physico-chemical characterization, exposure assessment, toxicology and bacteria resistance.[24]

Several works[19,25,26] revealed that AgNPs size is a critical parameter for the resulting biocidal properties indicating that the smaller the AgNPs, the stronger the antibacterial effect.[19,25] At high concentration, AgNPs might have a negative effect on the environment[27–29] and their addition in paint formulation could lead to dry-paint discoloration, low stability and inhomogeneities. Hence, AgNP aggregation must be avoided and a good AgNP dispersion is essential to ensure an efficient biocidal effect working with an AgNP content as low as possible. For this purpose, chemical capping agents or stabilizers (e.g., citrate, PVP)[30–32] are usually added during the AgNP synthesis to obtain well-dispersed NPs in aqueous medium. However, these agents can alter the Ag^+ ions release. A more "safer-by-design" and eco-friendly strategy can be actuated to fix them on a hydrophilic substrate that will promote the perfect dispersion in an aqueous medium. Since the oxidation process occurs at the surface, this approach should preserve the full biocidal efficiency of NPs with a reduction of the necessary AgNP amount in the system. Notably, a good AgNP dispersion can be reached by grafting AgNPs on a polysaccharide such as cellulose nanocrystals (CNCs) thus obtaining a biocidal hybrid partly bio-based NP[33–37]

In this work, we propose paint formulation strategies to reach high biocide efficiency while minimizing the risk at each stage of the life cycle, promoting a new safety-by-designed approach. The antibacterial properties are obtained by introducing well-dispersed hybrid NPs with AgNPs nucleated at surface of CNCs, in paint. The AgNP stabilization with CNCs allows simultaneously maximizing AgNP specific surface area without addition of any chemical capping agent and releasing cellulose in the environment after use. Paints were prepared using three different hybrid systems varying in CNC surface treatment and AgNP grafting method and then dried on specific supports. An artificial weathering is applied to simulate the paint deterioration caused by natural phenomena. Abrasion tests have been performed to obtain the particles emission in airborne from paints before and after artificial weathering scenarios. The life-cycle assessment was assessed for paint needed to cover 1 m^2 of wall during 10 years as a functional unit. The biocidal activity of dry-state paints has been checked by diffusion disk tests on *Bacillus subtilis* strain. Finally, toxicity of pristine NPs and abraded paints were assessed on A549 human lung epithelial cell line. Our results confirm that the use of hybrid CNC/AgNP system induces an effective biocidal effect on the dry paint.

MATERIALS and METHODS.

Chemicals. For the formulation of all the hybrid suspensions, commercial cellulose nanocrystals (CNCs) from CelluForce were used (length = 183 ± 88 nm; cross-section = 6 ± 2 nm; aspect ratio = 31).[38] Silver nitrate ($AgNO_3$, ≥ 99%), sodium borohydride ($NaBH_4$, ≥ 96%), (3-aminopropyl)triethoxysilane (APTES), toluene, ethanol, dimethylsulfoxide, diethylether, nitromethane, 1-bromopentane, hydrazine, sodium chloride (NaCl BioXtra grade 99%) were all purchased from Sigma-Aldrich (France) and used without further purification. 2-(4-pyridylethyl)triethoxysilane was acquired from ABCR (Germany). All the aqueous suspensions and solutions were prepared using ultra-pure water.

Synthesis of H1 hybrid using $NaBH_4$. The synthesis method of this system was carried following the experimental protocol proposed in another work of our group.[37,39] A volume of 500 mL of CNC suspension (15 g/L) was dialyzed against water for 3 days and then mixed with 25 mL of $AgNO_3$ aqueous solution (1 M). Then, 40 mL of freshly-prepared $NaBH_4$ aqueous solution (1 M) were gently added to the CNC/$AgNO_3$ aqueous suspension under stirring to reduce Ag^+ ions and synthetize AgNPs ($NaBH_4$/$AgNO_3$ molar ratio of 2). The CNC/AgNP suspension was put under stirring for 24 h at room temperature and finally dialyzed against water for 24 h. The samples were stored at 4°C in the dark.

Synthesis of H2 hybrid using hydrazine (N_2H_4). A detailed protocol and schematic representation of the experimental protocol are reported in S1.1. Briefly, the CNCs (10 g, 0.062 mol) were first surface-functionalized with NH_2 chelating groups by silanization with 3-aminopropyltriethoxysilane (APTES) in toluene (300 mL) at reflux, under stirring at 120 °C for 24 h according to the protocol proposed by Khanjanzadeha et al.[40]. The functionalized CNCs (i.e., A-CNC) were centrifuged (5000 rpm for 10 min), washed in ethanol and dialyzed against deionized water twice. A procedure to confirm the effective surface modification is represented in S1.2. Then, A-CNCs was mixed with a saturated solution of $AgNO_3$ in an ethanol/dimethylsulfoxide mixture (100 mL at 50/50 v/v). The resulting suspension was stirred for 4 h and washed in ethanol/dimethylsulfoxide. Finally, the chemical reduction of Ag^+ ions was performed using hydrazine (N_2H_4) in conditions to only reduce the silver ions effectively complexed on the CNC surface. The final product was finally washed in ethanol and water. The CNC concentration in the final suspension was 10 g/L. The samples were stored at 4°C in the dark.

Synthesis of H3 hybrid with AgBr. The experimental protocol was adapted from Sambhy et al.[21] The CNCs (10 g, 0.062 mol) were surface-functionalized with pyridyl chelating groups by silanization, working with 2-(4-pyridylethyl)triethoxysilane (5% molar with respect to CNC) in toluene at reflux for 24 h. The functionalized CNCs in suspension, named as P-CNCs, were centrifuged (5000 rpm for 10 min) and washed in ethanol and deionized water twice. The resulting P-CNCs were resuspended in

nitromethane with 1-bromopentane (5% molar with respect to CNC) under stirring at 60 °C for 24 h to produce quaternized analogue species. The resulting P^+-CNCs washed in ethanol and deionized water and dispersed in nitromethane was mixed with $AgNO_3$ dissolved in dimethylsulfoxide/nitromethane in 1:1 ratio and cooled to 0 °C. The $AgNO_3$ solution was then added dropwise to P^+-CNCs solution, and stirred for 1 h at room temperature to form AgBr/CNC complex species. The resulting suspension was washed in diethylether, ethanol and deionized water. The final hybrid sample was stored in the dark at 4°C. A detailed protocol is reported in S2.

Characterization of CNC/AgNP hybrid suspensions. The CNC/AgNP hybrids were all characterized by **scanning transmission electron microscopy** (STEM). The hybrids were diluted at 0.5 g/L and a volume of 10 μL was deposited onto glow-discharged carbon coated grids (200 meshes, Delta Microscopies, France) for 2 min. The excess of liquid was removed by blotting and the grids were dried overnight in air and then coated with 0.5 nm platinum layer by an ion-sputter coater. Images were recorded working with Quattro Scanning Electron Microscope (Thermo Fisher Scientific, USA) at 10 kV using a STEM detector. The analysis of the acquired images was performed by ImageJ software in order to determine the average AgNP Feret's diameter (i.e., the largest distance of two tangents to the contour of the measured particle), estimated considering 100 AgNPs for each sample.
Atomic Absorption Spectrometry (AAS) allowed evaluating the AgNP content in hybrids (ICE 3300 AAS, Thermo Fisher Scientific, USA). A volume of 1 mL of each suspension was digested by 40 mL water/aqua regia mixture overnight (i.e., 30%v aqua regia with HCl/HNO_3: 3/1) and then analyzed. A calibration curve was obtained using a silver standard solution (1000 μg/mL, Chem-Lab NV, Belgium) at different concentrations, from 0.25 to 15 ppm. Two independent measurements were performed for each sample.
UV-visible spectra were acquired by a Mettler-Toledo UV7 spectrophotometer (USA) equipped with a 10 mm quartz, working in the 300 – 900 nm range. All the samples were diluted (1:10) and ultra-pure water was used as a blank reference.
X-ray diffractograms (XRD) were recorded on a Bruker D8 Discover diffractometer (USA), with 10 acquisitions per minute. Cu Kα1 radiation (1.5405 Å) was produced in a sealed tube at 40 kV and 40 mA, parallelized using a Gobël mirror parallel optic system and then collimated to produce a 500 mm beam diameter. The data were collected in a 2θ angle range from 3° to 70°.

Paints formulation. All the paints were formulated and prepared by the manufacturer ALLIOS (France), following the preparation method proposed in the work of Rosset et al.[41]. Briefly, the organic-based paint was composed of an acrylic base (binder), micro-sized TiO_2 which provides the white color of the paint, calcium carbonate particles, aluminosilicate, water and other additives. Then, CNC/AgNP hybrid suspensions were incorporated in the paint. Some reference paints were also

formulated using unmodified CNCs or commercial biocides (i.e., AgCl, MIT, BIT, CIT). All the formulated paints are listed in Table 1 and they are characterized by a dry-matter content of 60%.
Finally, each paint was applied by an automatic film applicator (K Hand Coater, RK Print Instruments, UK) on standard supports, such as Taber (aluminum, Taber Industries, USA) and Leneta (black plastic-vinyl chloride/acetate copolymer with a smooth matt surface, Leneta Company, USA), obtaining a wet thickness of 100 µm for Taber and 150 µm for Leneta.

Table 1. Formulation of paints prepared using various amounts of commercial biocides or synthesized CNC/AgNP hybrids.

Sample	**Hybrid characteristics**	**Designation**	**Amount of biocide material (wt%)**	**Amount of Ag in paints (wt%)**
R0	-	Paint std without biocide	0% biocide	0%
CNC	Unmodified CNCs	Paint with CNC (no AgNP)	0% biocide	0%
R02	-	Paint std with organic commercial biocide (BIT/MIT/CIT)	0.2% organic biocide	BIT-100 ppm. MIT-100 ppm. CIT/MIT 2 ppm
AgCl0006	-	Paint with commercial biocide AgCl	0.3% Ag commercial biocide	0.006% AgCl
H1-0006	Unmodified CNC; AgNP synthesis by $NaBH_4$	Paint with H1 hybrid slurry – 0.25% AgNP in slurry;	2.00% hybrid	0.006% AgNP
H1-002			6.67% hybrid	0.02% AgNP
H1-004			13.33% hybrid	0.04% AgNP
H1-008			25.67% hybrid	0.08% AgNP
H2-002	CNC silanization by APTES; AgNP synthesis by hydrazine	Paint with H2 hybrid – 0.14% AgNP in slurry	14.39% hybrid	0.02% AgNP
H2-0035			25.67% hybrid	0.036% AgNP
H3-002	CNC silanization by 2-(4-pyridylethyl)triethoxysilane; AgBr synthesis	Paint with H3 – 0.13% AgNP in slurry	15.63% hybrid	0.02% AgNP
H3-0035			25.67% hybrid	0.033% AgNP

Biocide activity tests. For disk diffusion tests, the *Bacillus subtilis* strain was used (3610 strain, wild type, personal gift from Maria Laaberki). The cells were grown in Luria-Bertani (LB) medium: 10 g/L tryptone, 5 g/L yeast extract and 5 g/L NaCl. A 3610 *Bacillus subtilis* culture grown overnight on liquid LB at 37 °C was diluted to A_{600nm}= 0.1 in 10 mL of fresh LB medium and incubated at 37 °C and 200 rpm until the A_{600nm} reached the exponential phase (≈ 0.6). 300 µl of this culture (or 10^8 cells) were then uniformly applied on the surface of a LB agar plate (22 mL of LB-agar) before placing the different paints applied on Leneta support (5 mm diameter disk) on the plate. Positive and negative controls were tested on the same plate: 3 µl of ethanol 70% or H_2O, respectively, were applied on 5 mm paper disks (Blotting paper, grade 703 from VWR). The commercial organic biocide BIT/MIT/CIT mix was tested alone at different concentrations using the same approach: 3 µl of each dilution was applied on 5 mm paper disks. After 48 h at 30 °C, the average diameter of the inhibition zone was measured. The diameter of the inhibition halo was calculated from scanned images and subtracting the size of the disk diameter. Reference biocidal effect was obtained considering the antibacterial activity in liquid paints containing commercial biocides, such as AgCl (0.006 wt%) or commercial BIT/MIT/CIT agents at various concentrations (0.2 – 2 – 20 wt%). The dose response has also been assayed with a range of $AgNO_3$ and AgNPs (from 0.004 to 0.1 %) (Figure S.4.1). Two measurements were performed for each sample.

The artificial weathering of paints deposited on Leneta and Taber supports was performed in an accelerated weathering chamber (model QUV accelerated weathering, Q-Lab, USA) during 250 hours and 500 hours, according to the ISO 16474-3 standard. The paints underwent two different alternated cycles: i) exposure to UVB-313 lamps with irradiance of 0.71 $W.m^{-2}$ at 310 nm during 5 hours at temperature of 50 ± 3°C; ii) exposure to water spraying at a flowrate of 7 L/min during 1 hour at temperature of 25 ± 3°C without irradiation.

The surface morphology of paints deposited on Leneta support was observed by **ultra-High-Resolution Scanning Electron Microscopy** (HR-SEM, LEO 1530, UK) before and after artificial weathering. The paint samples were sputter-coated with a 10 nm thick platinum layer and all the images were collected working at an accelerating voltage of 5 kV, at a distance of 3.7 mm and with a diaphragm aperture of 30 µm. Before the artificial weathering treatment, the same samples were analyzed using **Scanning Electron Microscopy** coupled with **Energy Dissipation Spectroscopy** (SEM-EDS) method was used to investigate the composition of the dry-paints at the surface working with a Quattro Scanning Electron Microscopy (Thermo Fisher Scientific, USA) at 15 kV equipped an EDS detector (Bruker QUANTAX XFLASH 6|60, USA). For each sample, 3 million of counts were acquired and the size of the analyzed surface was 100 x 100 µm.

The abrasion tests were performed on dry paints on the Taber support (Scheme S1), with and without prior artificial weathering. Abrasion tests were performed according to the ISO 7784-2 standard. The

samples were placed in a glove box equipped with a HEPA filter with a background noise of less than 5 particles per cm^3. This condition was achieved by creating a vacuum at the top of the box which sucks the air at a rate of 150 L/min. Paint abrasion was performed in a Taber rotary abraser (model Abraser 5135, static mode, Taber industries, USA). An S42 abrasive paper was placed on the CS-0 type wheels to simulate the sanding process on the surface. A weight of 500 g was applied on both wheels during 200 cycles at 60 rpm. During the experiment, a flow splitter connected to a sampling rod was placed 10 mm away from one of the two abrasion wheels in order to collect the particles released. The airborne particle concentration was recorded in real time with a condensation particle counter (CPC, model 3775, TSI Incorporated, USA). The CPC measured the aerosol particle size ranging from 5 nm to 3 µm. Aerosolized particles were collected on a filtration system composed of a hydrophilic polycarbonate membrane (PCM, Millipore, USA) with a pore size of 0.4 µm. The deposited emitted particles were characterized by scanning electron microscopy coupled with energy dispersion X-ray spectroscopy (HR-SEM-EDS).

Life cycle assessment (LCA) was performed according to the ISO standard 14040 and 14044, following ILCD guidelines, on a so-called "white" base. This 4-step method allows converting the input and output to the investigated system into quantified impacts on the environment. This conversion is called impact characterization and it was performed using the SimaPro software® (Netherland, 2.8 version). A cradle-to-grave perimeter was assessed, including transport and unused paint end of life but excluding the end of life of the applied paint on walls. The selected functional unit corresponded to the amount of paint required to cover 1 m^2 of wall for 10 years. The inventory was collected from the paint manufacturer and modelled using Ecoinvent database V3.5 (system model allocation, recycled content). For material not characterized in the Ecoinvent database, such as biocides, a mixture of alternative equivalent chemicals was modelled, based on usual commercial biocide composition. The simulated scenario considered all the precursors necessary for paint production (i.e., from the extraction of the resources to the production of all paint components) as well as the stages after their application up to end of life, other than recycling. The environmental impact associated to global warming, human toxicity, terrestrial eutrophication, fresh water eutrophication and marine eutrophication, was calculated using ILCD 2011 Midpoint+ characterization method (1.08 version), as recommended by European Commission.

Potential pulmonary impact of abraded paints particles and NP

In order to evaluate potential pulmonary impact of abraded paint residues and the pristine NP used in these paints, cytotoxicity, oxidative stress and inflammation were assessed on A549 cell line. These endpoints have been chosen since these biological effects have already been described for CNC. 47 A549 cells were chosen because they are a well-studied and described model to study pulmonary toxicity in vitro. Cell culture conditions and toxicity assays protocols are detailed in SI (S8).

Preparation of abraded paints residues and NP suspensions. For exposures, abraded paints residues were suspended in ultrapure water at 1 mg/ml. In order to reduce particles size, abraded paints were sonicated with a microtip (at 100% for 2 minutes, 1 sec ON, 1 sec OFF). These abraded paints dispersions were diluted in cell culture media at 50, 100 et 500 µg/mL. Native CNC and H1 hybrid (H1-008 from table 1) were already in suspension in water, thus were just further diluted in cell culture media et 10, 50 et 100 µg/mL. TiO_2 P25 (Evonik) NPs, used as a positive NP control in the oxidative stress experiment, was suspended in water at 1 mg/ml in ultrapure water, then sonicated with a cuphorn (sonicator S-4000, Qsonica ; at 4°C ; amplitude 40 ; 5', 30s ON, 15s OFF) and then diluted in culture media at 100 µg/ml.

Statistical analysis. For each experiment, cells are exposed in triplicates. Mean of these triplicates are used for calculations. Three different experiments are used to evaluate cell responses and for statistical analysis using GraphPad Prism 8. Two ways ANOVA and Dunett post-hoc were performed. P-value was considered significative below 0.05.

RESULTS and DISCUSSION.

Characterization of CNC/AgNP hybrids. Various strategies can be used to fixe AgNPs on CNC surface that are more or less impacting. Three of them were chosen for their differences in final structure and not onin synthesis, in order to study the impact of both grafting (chemical or physical) and structure (crystal or amorphous) on biocidal activity;

H1 is grafted with of AgNPs on the surface of the unmodified CNCs by direct interaction between the Ag^+ ions and the CNC surface hydroxyl groups.[42] CNCs acted as stabilizers ensuring the AgNP well-dispersion, as proved by STEM image (Figure 1) and by the presence of a well-defined peak at 395 nm in the UV-Vis spectra (Figure S3a). The XRD diffractograms of the AgNPs in H1 hybrid (Figure S3b) displayed peaks at 38°, 44° and 64° that correspond to the (111), (200) and (220) Ag plans, respectively. This clearly identified a face-centered cubic (fcc) silver structure with the isotropic nature of the crystals[35] (JCPDS Card No. 89-3722).

H2 provided AgNPs with a fcc crystalline structure identified by XRD. Most of them appeared grafted on the APTES-CNC surface and quite well-dispersed. Indeed, a peak appeared in the UV-Vis spectra at 415 nm (Figure S3a), as observed for the $NaBH_4$ system, but wider and with a higher baseline compared to the H1 case. This underlines an increase of AgNP polydispersity.

H3 was prepared without reduction step, but containing the biocidal AgBr salt, the characteristic peaks were not observed in the XRD diffractogram indicating that AgNPs did not show a fcc structure. This is in accordance with the chemical nature of AgBr that don't form AgNP composed by Ag_0 but an Ag^+ complexation and precipitation. Moreover, some AgBr objects in H3 not grafted on CNCs surface were observed by STEM (Figure 1). Also, its UV-Vis spectrum (Figure S3a) did not show the

characteristic peak around 400 nm and the increase of the baseline intensity revealed a possible polydispersity or aggregation.

The three hybrids are then characterized as:

- H1 hybrid: no surface-modification pretreatment of the CNC, and Ag^+ ions issued from AgNO3 are reduced using $NaBH_4$, leading to a content of 25 wt% of crystalline AgNPs of 11± 9 nm homogeneously distributed on the CNC surface;
- H2 hybrid: CNCs were surface-modified by APTES and the Ag^+ ions issued from AgNO3 are reduced using hydrazine, leading to a content of 14 wt% of crystalline AgNPs of 42± 23 nm,
- H3 hybrid: CNCs were surface-modified using 2-(4-pyridylethyl)triethoxysilane and the AgBr precipitation occurred on the quaternized amino moieties. It presents un-crystallized AgNPs of 48 ± 29 nm nm with a content of 13 wt%.

The size distributions of AgNPs in the various hybrid systems are reported in Figure S3c.

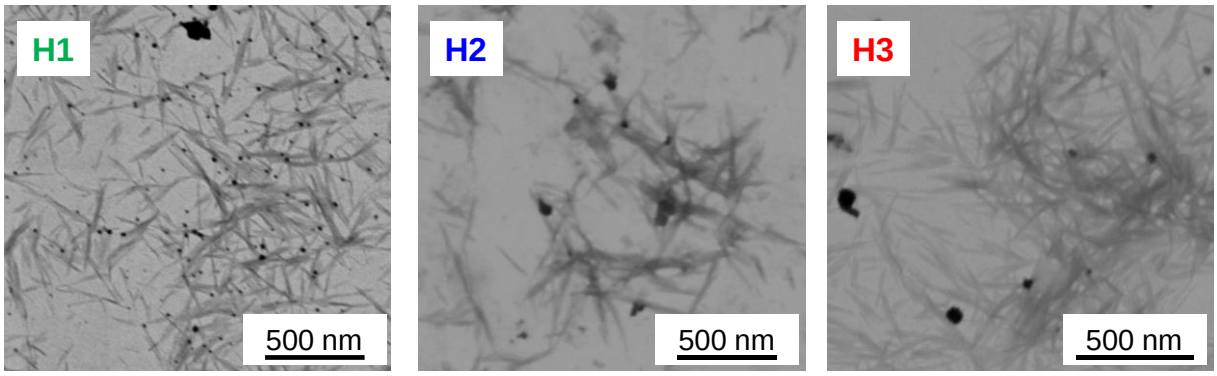

Figure 1. STEM images of dry H1, H2 and H3 hybrids.

Biocidal efficiency of paints. The biocide effects were assessed on the bacterium *Bacillus subtilis* which is the standard model of Gram positive bacteria. Its natural biotope is the upper layer of the soil but it is also more and more found in the gastrointestinal tract of mammalian or breed animals as chicken or shrimp. This bacterium is completely safe for human and animal health. The biocide efficiency of dry-film paints was determined from the diameter of the inhibition halo on a *Bacillus subtilis* strain measured after 48 h at 30 °C. As shown in Figure 2a, the dry-state paints formulated with AgCl at the commercial usual concentration of 0.006 wt% (AgCl0006) and the one formulated using a commercial organic biocide BIT/MIT/CIT at 0.2 wt% (R02) did not provide a biocidal activity. This result suggested that BIT/MIT/CIT biocidal agent did not ensure an antimicrobial activity in the dried paint. It was checked that paint formulated with only CNC did not provide any detectable biocidal effect. On the other hand, the three dry-state paints formulated with the hybrid systems at the same Ag content of 0.02 wt% could detect antimicrobial activity. To quantitatively describe the biocidal effect of the dry-state paints formulated with H1, H2 or H3 hybrids, a calibration curve for the antibacterial activity was prepared measuring the inhibition halo of BIT/MIT/CIT

commercial agent at three concentrations (0.2 – 2 – 20 wt% Ag) in the same condition, Figure 2b. The comparison of H1-002 paint (containing 0.02 wt% Ag) with the reference curve shows a biocide effect equivalent to a formulation containing a commercial biocide content of 0.2 wt%. It followed that the presence of well-dispersed AgNPs nucleated on CNC surface allowed reducing the overall Ag content 10 times in the paint to obtain the same efficient biocidal activity in the dry-state paint, contrary to what happens with AgCl0006 and R02 paints. However, no antimicrobial activity was recorded at 0.006 wt% Ag using H1 hybrid (i.e., H1-0006, Figure 2b), defining the critical Ag content between 0.006 wt% and 0.02 wt% to obtain a measurable biocidal effect on dry paint. Conversely, paint formulated with H2 hybrid (i.e., H2-002 inhibition halo of 0.14 mm) displayed no biocidal activity, and H3 hybrid showed an antimicrobial effect just above the detection limit (i.e., inhibition halo of 1.55 mm), Figure 2a. The diffusion disk images of paints formulated with different CNC/AgNP hybrid systems are shown in the inset of Figure 2a and Figure S4.2. In the case of paints containing the H2 hybrid, the absence of biocide activity can be related to the unperfect dispersion of CNCs, and thus of the AgNPs, in the initial suspension (Figure 1). Moreover, it could be also hypothesized that residual hydrazine remained complexed at the AgNP surface thus affecting the Ag^+ release kinetics. The paint formulated with the H3 hybrid showed a reduced biocidal activity which could be related to the presence of Br^- ions associated to an inefficient AgBr dissolution. Indeed, while for AgNPs synthetized in the H1 and H2 systems, the Ag^+ release derived from the AgNP oxidation, in the H3 the biocidal activity was mainly associated to the dissolution of the precipitated AgBr. Moreover, it is known that AgNP size strongly affects the consequent biocidal effect since the increased specific surface (as in the case of smaller AgNPs) leads to stronger biocidal activity.[18,19,25] Thus, the reduced biocidal activity of paints using H2 and H3 samples could be also linked to the higher average diameter of their AgNPs (i.e., 42 ± 23 nm and 48 ± 29 nm, respectively) compared to the H1 hybrid (i.e., 11 ± 9 nm). Considering these results, H1 system with the smallest AgNP dimension seems the most promising.

Furthermore, Figure 2b shows that the increase of Ag content in H2 and H3 in dry-state paints did not allow an increase of the inhibition halo size (i.e., inhibition halo of H2-002 and H2-0035 equal to 0.14 mm and 0.22 mm, respectively; inhibition halo of H3-002 and H3-0035 equal to 1.55 mm and 1.49 mm, respectively). The images of diffusion disks used for biocide tests are reported in Figure S4.2.

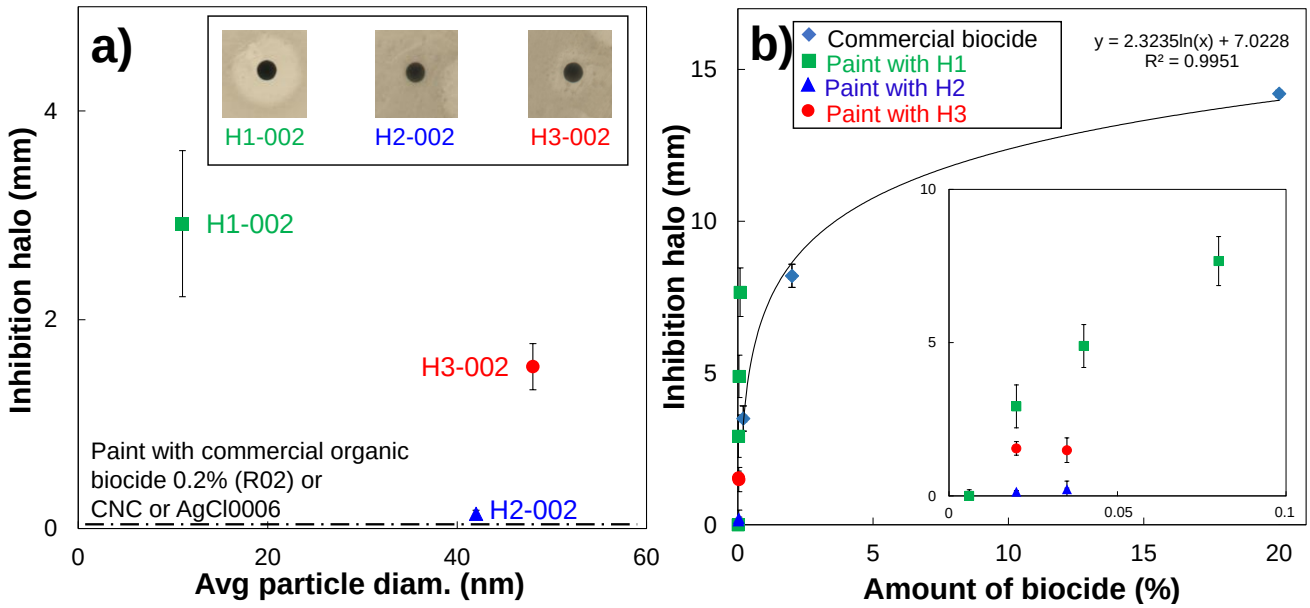

Figure 2. a) Inhibition halo of paints at 0.02% Ag formulated with different hybrid systems. Inset: diffusion disks. b) Calibration curve obtained considering the inhibition halos of commercial biocide at various contents. Inset: Inhibition halos of paints at various Ag contents formulated with various hybrid suspensions.

On the other hand, the same increase of the Ag content with H1 hybrid induced a clear increase of the inhibition halo (i.e., 2.9 ± 0.7 mm, 4.9 ± 0.7 mm and 7.7 ± 0.8 mm for paints containing 0.02 wt% (H1-002), 0.04 wt% (H1-004) and 0.08 wt% (H1-008) Ag, respectively). These results underlined how the well-dispersed smaller AgNP grafted on CNCs allowed obtaining a highly efficient antimicrobial activity. Furthermore, SEM-EDS measurements (Figure S5a and S5b) showed that the intensity of the characteristic peak at 3 KeV commonly associated to the surface plasmon resonance of AgNPs increased with the increase of the Ag content, suggesting that the CNC/AgNP did not specifically migrate to the paint surface during the drying step. Such experimental evidence can predict a long term active biocidal property since the AgNPs are also distributed in the core of the dry-state paint and efficient even for a very low amount of Ag compared to commercial biocides. These results strongly support that the final product will be washable without losing activity, and the intensity of the biocidal effect can be easily tuned just varying the hybrid content in the formulation.

An important aspect of the life cycle of a product such as a paint is to determine its durability, i.e., to evaluate whether the added NPs can be released after aging and/or during abrasion. Abrasion is a key stage in the life cycle because it simulates the moment when a person could inhale aerosols potentially containing added NPs that is classically identified as the worst exposure route for health.

Artificial weathering of dry paint. Native CNC and hybrids were introduced in various amounts in a real paint formulation and compared to paint prepared with 0.2 wt% of commercial organic biocide or 0.3 wt% of AgCl (Table 1), homogeneously applied on a model surface and allowed to dry for three

weeks. The paints were further submitted to two alternated cycles: i) exposure to UVB during 5 hours at 50 °C and ii) exposure to water spraying during 1 hour at 25 °C. The surface of each paint was photographed before and after 250 and 500 h of artificial weathering (Figure S6). No visible impact on the quality of the paint film was observed in all the conditions. However, some slight yellowing after 500 h of UV exposure were observed for standard paints formulated without any biocide or with native CNCs, as for paints prepared with 0.2 wt% of organic biocide or 0.006 wt% of AgCl biocide (inset Fig 3). Paints formulated with H1 hybrid became browner when the amount of AgNP and/or the UV exposure duration increased. Paints formulated with the H2 or H3 hybrids turned on a pale yellow even after 500 h of UV exposure. To better shed light on the impact of the artificial weathering on the paint color variation, the morphology of paints before and after 500 h of exposure to artificial weathering was investivated by HR-SEM. Figure 3 compares HR-SEM images before and after artificial weathering for the reference paint without biocide (R0) and paints containing hybrids H1, H2 and H3 including 0.02 wt% Ag. Before artificial weathering, the particles seem to be covered by a thin organic matrix layer (Figure 3, upper line). On the other hand, after 500 hours of exposure (Figure 3, bottom line), this thin organic matrix layer was maintained for the R0 paint (without biocide) but removed for the three other paints. Thus, a photodegradation of the organic matrix seemed to occur during the UV exposure inducing an increase of the AgNP mass fraction at the paint surface, resulting in a paint color change. Our observations agreed with previous studies that reported that the organic matrix of paints formulated with SiO_2 and TiO_2 nanoparticles can be degraded by artificial weathering,[43,44] leading to the photodegradation of the polymeric matrix by UV light and to an accumulation of SiO_2 nanoparticles at the surface. However, these results are strictly limited to the paint surface with a large fraction still present deeper in the paint.

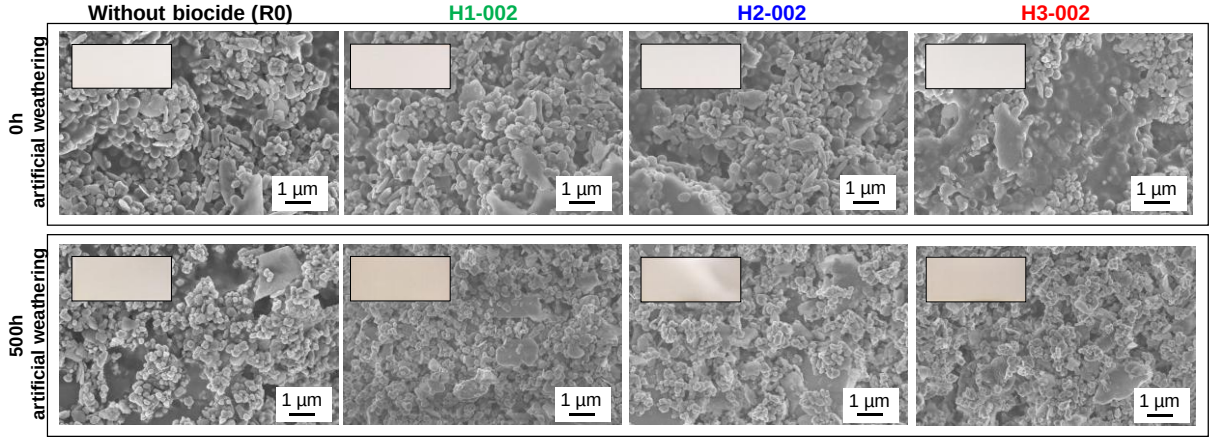

Figure 3. HR-SEM images of paints formulated without biocide and paints at 0.02wt% Ag formulated with H1, H2 and H3 hybrids, before (upper line) and after 500 hours (bottom line) of exposure to artificial weathering. The inset of each image represents a macroscopic picture of the corresponding paint.

Wheels abrasion tests were carried out during 200 cycles at 60 rpm. The paint particles emitted during the abrasion were measured by a CPC between 5 nm and 3 µm. As shown in Figure 4a, a

significant difference between concentration of the emitted particle of the reference paints R0 and CNC, compared to that of the paints formulated with the three CNC/AgNP hybrids at various concentrations. Before artificial weathering, the R0 and CNC paints released 20 times more particles during the abrasion than paints containing CNC/Ag hybrids. Interestingly, the particle emission decreases with the increase of artificial weathering time, as similarly observed by Rosset et al.[41] Such a behavior can be related to the degradation of the paint by UV light, which induced detrimental paint properties leading to the emission of bigger aggregates during the abrasion process. Because of their size, it could be supposed that these aggregates were probably out of the CPC measurement range. Oppositely, the addition of CNC/AgNP hybrid in the formulation decreased the particle emissions during the abrasion before and after artificial weathering. For all these hybrid paints, the measured particle concentration was lower than the background noise of 5 particles per cm^3, except for H1 paint with Ag at 0.04 wt% after 250 h of UV exposure which is most probably artefactual. It can be highlighted that the addition of hybrids in paint formulation decreased the number of emitted particles in the CPC range, independently from artificial weathering and from the hybrid synthesis. Finally, the paint formulated with the commercial organic biocide (R02) generated more emitted particles compared to the paint with commercial mineral biocide (AgCl0006) during the abrasion process, irrespective from the artificial weathering. Thus, the mineral biocide (AgCl) in the paint formulation seemed to limit the airborne particles emissions compared to an organic biocide (R02). It resulted that the addition of hybrids in paint formulation decreased the emission of particles in the CPC range, regardless of the artificial weathering or the hybrid synthesis condition.

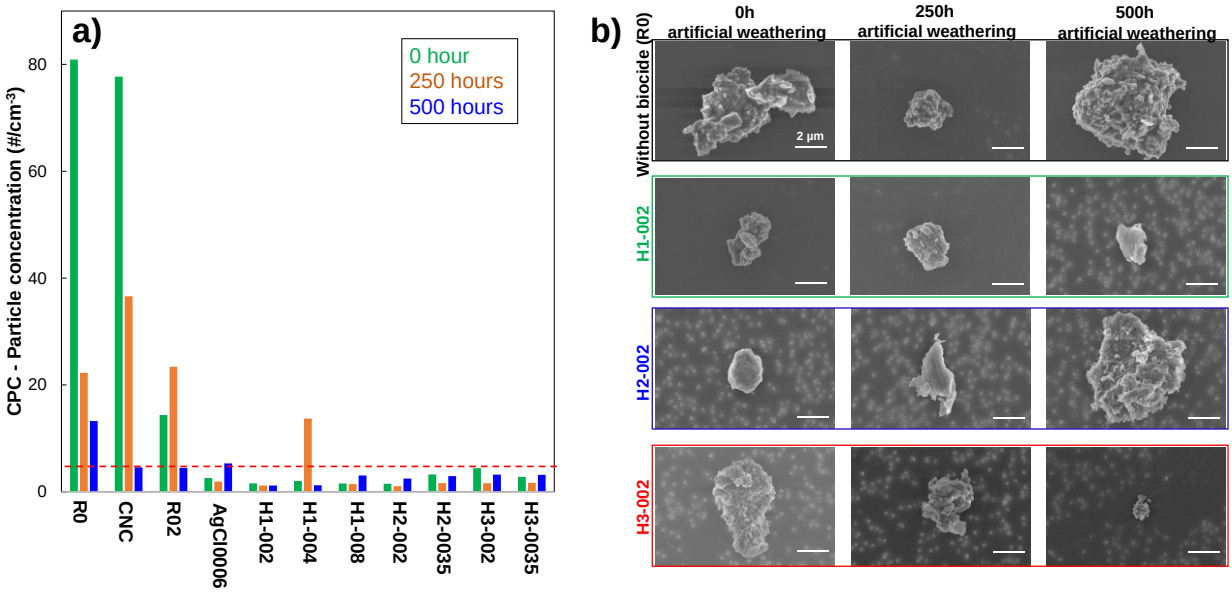

Figure 4. a) Particle concentration from 5 nm to 3 µm released per cm^3 measured by CPC before (green) and after 250 hours (orange) and 500 hours (blue) of artificial weathering exposure. The red line represents the background noise level. b) SEM images of particles released after abrasion tests by R0, H1-002, H2-002 and H3-002 paints before and after 250 and 500 hours of UV exposure. For all the images, the scale bar is 2 µm.

During the abrasion tests, paint particles released in air were collected on a hydrophilic polycarbonate membrane. SEM analysis with elementary chemical composition was performed on the particles released during the abrasion from paints R0, H1-002, H2-002 and H3-003 before and after different artificial weathering times. SEM images show the presence of micrometric agglomerates with a size ranging from 2 to 7 μm composed of carbon, oxygen, magnesium, aluminum, silicon, calcium, titanium and platinum, as indicated by EDS analysis (Figure S7). It confirms that the agglomerates released in air from paints before and after artificial weathering during the abrasion were originating from paint fragments. No free AgNPs were identified. These results agreed with numerous literature studies which show that the emitted particles were linked to the matrix.[43,45,46] On the other hand, the artificial weathering does not affect the shape, size and chemical composition of paint aerosols released into air during the abrasion. It is important to note that the overall nanoparticles emissions from paints are very low. Thus, such paint formulation does not affect the worker and the environment during a sanding step from point of view of nanomaterials released.

LCA analysis. Finally, the environmental impact was assessed, considering a paint with a so-called *white* base containing a mixture of two oxidizing agents (i.e., chlorine dioxyde and hydrogen peroxide) and two highly toxic organic substances (i.e., dithiocarbamate and cyanazine). The biocide concentration in paint was fixed equal to 0.0015 wt% according to the threshold limit of MIT biocide defined by European Chemicals Agency (ECHA). The outcomes of the LCA analysis are shown in Figure 5. It resulted that the paint manufacturing represents 65% to 90% of the overall impact of the paint life cycle, for all impact categories (i.e., global warning, human toxicity, terrestrial eutrophication, fresh water eutrophication and marine eutrophication). Thus, relevant efforts should be directed towards reducing the use of toxic solvents and resins during the paint fabrication, replacing them with greener products in the framework of a safer-by-design approach. However, the current life cycle analysis models are limited and they do not yet consider the additional impacts related to the use of nanometric objects.

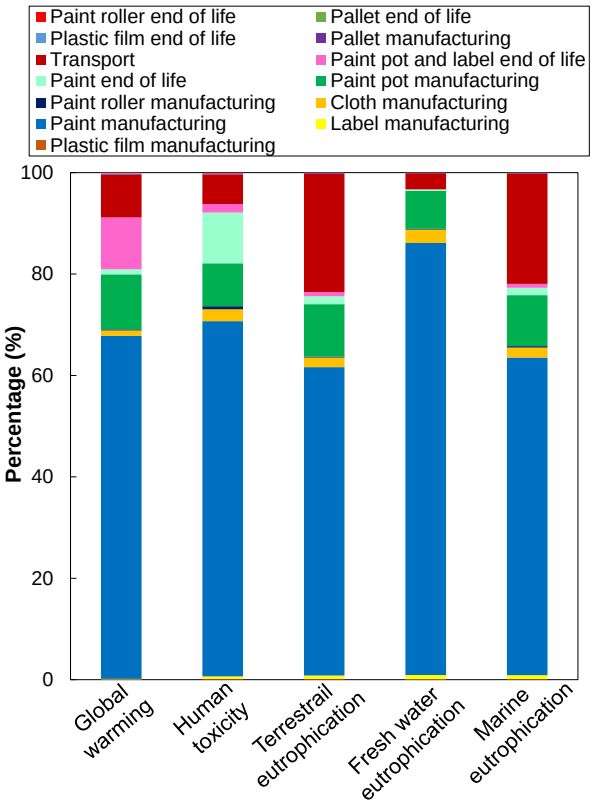

Figure 5. Impact of the different life cycle steps on the different impact categories for the manufactured white based paint with biocide.

Toxicity results. Tests performed on abraded paint after NPs (CNC or CNC/Ag) exposure showed no cytotoxicity or very low viability loss (below 20 %) (Figure S8a) even at the highest dose tested (100 µg/mL). However, a clear cytotoxicity was observed after exposure at the highest tested dose (500 µg/mL) either with the Taber support, or abraded paints with or without CNC or CNC/AgNP (from 39 % to 65 %). This cytotoxicity might be an unspecific cell response due to a very large tested dose. Medium and low doses of Taber and paint without CNC induced no or a slight cytotoxicity. However, a low cytotoxicity (between 30% and 15 %) after medium and low dose exposures of abraded paints with CNC and CNC/AgNP was noticed, but there was no difference with or without Ag. Thus, CNC and hybrids CNC/Ag could be responsible of a very low cytotoxicity of paints residues.

No ROS generation was measured after NPs exposure, except for TiO_2 positive control and chemical positive control. For abraded paints, some ROS was measured only after exposure to the highest dose for paints with CNC and CNC/Ag paints, at similar levels (Figure S8b). This result is unexpected since NPs by themselves did not induce ROS generation, but might be due to the dispersion procedure applied to break large particles only in abraded paint samples. Indeed, sonication process might have created ROS in paints with CNC and CNC/AgNP as shown in literature.[47]

A light inflammatory response was observed after exposure to the highest dose of CNC and CNC/Ag (Figure S8c). Unexpectedly, AgNPs on CNC seemed to decrease slightly the inflammatory response.

Similarly, abraded paints with CNC induced an inflammatory response higher than paints with CNC/AgNP hybrids. Thus, Ag seemed to reduce inflammation when associated with CNC either before or after inclusion in paint. However, a clear dose-response inflammation was noticed after exposure to abraded paint without CNC. Comparatively, CNC and CNC/AgNP seem to reduce inflammation of abraded paint, even more for paint including CNC/AgNP. This lower inflammation after exposure to abraded paints with CNC and CNC/AgNP could be because particles from these paints are smaller than paints without CNC (38 µm and 40 µm diameter for paints with CNC and CNC/AgNP respectively and 29 µm for paint without CNC, median diameter were measured by laser granulometry). Overall, AgNPs hybridized on CNC did not increased toxicity even after inclusion in abraded paints, on the contrary since they seemed to decrease inflammatory response on tested lung epithelial cells.

CONCLUSIONS.

The purpose of this work was to develop a global safe-by-design approach to formulate paint with high antimicrobial activity and lowest footprint on human health and environment. Silver nanoparticles were chosen for their high efficiency and low toxicity. AgNPs were fixed on the surface of cellulosic-based colloidal particles without the use of additional stabilizers, well dispersed in an aqueous media. Firstly, we synthetized three CNC/AgNP hybrid that differed by CNC surface modification and AgNP synthesis method. The average AgNP diameter varied from about 11 ± 9 nm for the H1 case up to 40-50 nm for the H2 and H3 systems. Their inclusion in the formulation of realistic paints allowed obtaining dry-films perfectly similar to original commercial paints. The characterization of the three paints before and after artificial weathering showed that CNC/AgNP hybrids induced slight degradation of the organic matrix in harsh conditions, as viewed by SEM, but also reduced the emission of airborne particles through mechanical solicitation. It should be noticed that only paint fragments were emitted in air during the abrasion process and no NPs were detected. However, the paint life cycle assessment was not relevant to identify the impact of such bio-based substrates due to their low amount revealing the limitation of such LCA for nanoparticles. Finally, biocidal activity was detected for the paint in wet state as well as in dry-films. The highest biocide effect was achieved with the smallest and best dispersed AgNPs (i.e., 11 nm in H1 hybrid), clearly indicating that the specific surface of AgNPs plays a crucial role in the resulting antibacterial efficiency. Indeed, in comparison, the other paints with AgNPs of about 40-50 nm displayed a biocide activity just above the detection limit. Furthermore, the biocidal activity of the paint formulated with H1, prepared from AgNO3 and reduced, included at 0.02 wt% Ag content, resulted equivalent to the one of commercial biocide content at 0.17 wt%. Thus, an efficient antimicrobial property was provided with much lower Ag amount. Also, toxicity tests showed that CNC/AgNPs did not increase toxicity but seemed rather to decrease inflammatory response.

Finally, we obtained tunable biocide efficiency in dry-state paint varying the amount of H1 hybrid This complete study leads to formulation allowing a fine control of the overall AgNP content to the just necessary without detrimental impact on the antimicrobial activity. Moreover, at the end of the paint life, and thus after the Ag^+ ion release, it is the CNC biodegradable substrate that persists in the paints, preserving from toxicity the material to be released in environment. This thus opens the road to the production of new safer-by-design paints and coating for wall, furniture or any surface that should be protected from biological attack.

ACKNOWLEDGEMENTS.

We gratefully acknowledge F. X. Lefevre and N. Guichard (Université de Nantes) for support in AAS experiments, B. Pontoire (BIA-Nantes) for performing XRD acquisitions, B. Novales (BIA-Nantes) for the STEM images acquisition. This work is a contribution to the Labex SERENADE (n° ANR-11-LABX-0064) funded by the "Investissement d'Avenir" French Government program of the French National Research Agency (ANR) through the A*MIDEX project (n° ANR-11-IDEX-0001-02).

REFERENCES

(1) Hochmannova, L.; Vytrasova, J. Photocatalytic and Antimicrobial Effects of Interior Paints. *Prog. Org. Coatings* **2010**, *67* (1), 1–5. https://doi.org/10.1016/j.porgcoat.2009.09.016.

(2) Bechtold, M.; Valério, A.; Ulson de Souza, A. A.; de Oliveira, D.; Franco, C. V.; Serafim, R.; Guelli, S. M. A. Synthesis and Application of Silver Nanoparticles as Biocidal Agent in Polyurethane Coating. *J. Coatings Technol. Res.* **2020**. https://doi.org/10.1007/s11998-019-00297-0.

(3) Tornero, A. C. F.; Blasco, M. G.; Azqueta, M. C.; Acevedo, C. F.; Castro, C. S.; López, S. J. R. Antimicrobial Ecological Waterborne Paint Based on Novel Hybrid Nanoparticles of Zinc Oxide Partially Coated with Silver. *Prog. Org. Coatings* **2018**, *121* (March), 130–141. https://doi.org/10.1016/j.porgcoat.2018.04.018.

(4) Machado, G. E.; Pereyra, A. M.; Rosato, V. G.; Moreno, M. S.; Basaldella, E. I. Improving the Biocidal Activity of Outdoor Coating Formulations by Using Zeolite-Supported Silver Nanoparticles. *Mater. Sci. Eng. C* **2019**, *98* (257), 789–799. https://doi.org/10.1016/j.msec.2019.01.040.

(5) Bogdan, S.; Deya, C.; Oscar, M.; Bellotti, N.; Romagnoli, R. Natural Products to Control Biofilm on Painted Surfaces. *Pigment Resin Technol. Artic. Inf. ester nanocomposites* **2017**.

(6) Kalishwaralal, K.; BarathManiKanth, S.; Pandian, S. R. K.; Deepak, V.; Gurunathan, S. Silver Nanoparticles Impede the Biofilm Formation by Pseudomonas Aeruginosa and Staphylococcus Epidermidis. *Colloids Surfaces B Biointerfaces* **2010**, *79* (2), 340–344. https://doi.org/10.1016/j.colsurfb.2010.04.014.

(7) Obidi, O.; Okekunjo, F. Bacterial and Fungal Biodeterioration of Discolored Building Paints in Lagos, Nigeria. *World J. Microbiol. Biotechnol.* **2017**, *33* (11), 1–9. https://doi.org/10.1007/s11274-017-2362-y.

(8) Kappock, P. S. Biocides: Wet State and Dry Films. In *Handbook of Coating Additives*; Florio, J. J., Miller, D. J., Eds.; Marcel Dekker, Ink, 2004.

(9) Gaylarde, C. C.; Morton, L. H. G.; Loh, K.; Shirakawa, M. A. Biodeterioration of External Architectural Paint Films - A Review. *Int. Biodeterior. Biodegrad.* **2011**, *65* (8), 1189–1198. https://doi.org/10.1016/j.ibiod.2011.09.005.

(10) Decraene, V.; Rampaul, A.; Parkin, I.; Petrie, A.; Wilson, M. Enhancement by Nanogold of the Efficacy of a Light-Activated Antimicrobial Coating. *Curr. Nanosci.* **2009**, *5* (3), 257–261. https://doi.org/10.2174/157341309788921561.

(11) Fulmer, P. A.; Wynne, J. H. Development of Broad-Spectrum Antimicrobial Latex Paint Surfaces Employing Active Amphiphilic Compounds. *ACS Appl. Mater. Interfaces* **2011**, *3* (8), 2878–2884. https://doi.org/10.1021/am2005465.

(12) Edge, M.; Allen, N. S.; Turner, D.; Robinson, J.; Seal, K. The Enhanced Performance of Biocidal Additives in Paints and Coatings. *Prog. Org. Coatings* **2001**, *43* (1–3), 10–17. https://doi.org/10.1016/S0300-9440(01)00244-2.

(13) Silva, V.; Silva, C.; Soares, P.; Garrido, E. M.; Borges, F.; Garrido, J. Isothiazolinone Biocides: Chemistry, Biological, and Toxicity Profiles. *Molecules* **2020**, *25* (4). https://doi.org/10.3390/molecules25040991.

(14) Basketter, D. A.; Gilmour, N. J.; Wright, Z. M.; Walters, T.; Boman, A.; Lidén, C. Biocides: Characterization of the Allergenic Hazard of Methylisothiazolinone. *J. Toxicol. - Cutan. Ocul. Toxicol.* **2003**, *22* (4), 187–199. https://doi.org/10.1081/CUS-120026299.

(15) Herman, A.; Aerts, O.; de Montjoye, L.; Tromme, I.; Goossens, A.; Baeck, M. Isothiazolinone Derivatives and Allergic Contact Dermatitis: A Review and Update. *J. Eur. Acad. Dermatology Venereol.* **2019**, *33* (2), 267–276. https://doi.org/10.1111/jdv.15267.

(16) Bottero, J. Y.; Rose, J.; De Garidel, C.; Masion, A.; Deutsch, T.; Brochard, G.; Carrière, M.; Gontard, N.; Wortham, H.; Rabilloud, T.; Salles, B.; Dubosson, M.; Cathala, B.; Boutry, D.; Ereskovsky, A.; Auplat, C.; Charlet, L.; Heulin, T.; Frejafon, E.; Lanone, S. SERENADE: Safer and Ecodesign Research and Education Applied to Nanomaterial Development, the New Generation of Materials Safer by Design. *Environ. Sci. Nano* **2017**, *4* (3), 526–538. https://doi.org/10.1039/C6EN00282J.

(17) Marambio-Jones, C.; Hoek, E. M. V. A Review of the Antibacterial Effects of Silver Nanomaterials and Potential Implications for Human Health and the Environment. *J. Nanoparticle Res.* **2010**, *12* (5), 1531–1551. https://doi.org/10.1007/s11051-010-9900-y.

(18) Ouay, B. Le; Stellacci, F. Antibacterial Activity of Silver Nanoparticles : A Surface Science Insight. *Nano Today* **2015**, *10* (3), 339–354. https://doi.org/10.1016/j.nantod.2015.04.002.

(19) Morones, J. R.; Elechiguerra, J. L.; Camacho, A.; Holt, K.; Kouri, J. B.; Ramírez, J. T.; Yacaman, M. J. The Bactericidal Effect of Silver Nanoparticles. *Nanotechnology* **2005**, *16* (10), 2346–2353. https://doi.org/10.1088/0957-4484/16/10/059.

(20) Kumar, A.; Vemula, P. K.; Ajayan, P. M.; John, G. Silver-Nanoparticle-Embedded Antimicrobial Paints Based on Vegetable Oil. *Nat. Mater.* **2008**, *7* (3), 236–241. https://doi.org/10.1038/nmat2099.

(21) Sambhy, V.; MacBride, M. M.; Peterson, B. R.; Sen, A. Silver Bromide Nanoparticle/Polymer Composites: Dual Action Tunable Antimicrobial Materials. *J. Am. Chem. Soc.* **2006**, *128* (30), 9798–9808. https://doi.org/10.1021/ja061442z.

(22) Ahmed, S.; Ahmad, M.; Swami, B. L.; Ikram, S. A Review on Plants Extract Mediated Synthesis of Silver Nanoparticles for Antimicrobial Applications: A Green Expertise. *J. Adv. Res.* **2016**, *7* (1), 17–28. https://doi.org/10.1016/j.jare.2015.02.007.

(23) Ferdous, Z.; Nemmar, A. *Health Impact of Silver Nanoparticles: A Review of the Biodistribution and Toxicity Following Various Routes of Exposure*; 2020; Vol. 21.

https://doi.org/10.3390/ijms21072375.

(24) ANSES - French Agency for Food and Environmental and Occupational Health & Safety. Exposure to silver nanoparticles: update of knowledge https://www.anses.fr/en/content/exposure-silver-nanoparticles-update-knowledge.

(25) Espinosa-Cristóbal, L. F.; Martínez-Castañón, G. A.; Martínez-Martínez, R. E.; Loyola-Rodríguez, J. P.; N. Patiño-Marín; Reyes-Macías, J. F.; Ruiz, F. Antibacterial Effect of Silver Nanoparticles against Streptococcus Mutans. *Mater. Lett.* **2009**, *63* (29), 2603–2606. https://doi.org/10.1016/j.matlet.2009.09.018.

(26) G. A. Martínez-Castañón, N. Niño-Martínez, F. Martínez-Gutierrez, J. R. Martínez-Mendoza, F. R. Synthesis and Antibacterial Activity of Silver Nanoparticles with Different Sizes. *J. Nanoparticle Res.* **2008**, 1343–1348. https://doi.org/10.1007/s11051-008-9428-6.

(27) León-Silva, S.; Fernández-Luqueño, F.; López-Valdez, F. Silver Nanoparticles (AgNP) in the Environment: A Review of Potential Risks on Human and Environmental Health. *Water. Air. Soil Pollut.* **2016**, *227* (9). https://doi.org/10.1007/s11270-016-3022-9.

(28) Panyala, N. R.; Peña-Méndez, E. M.; Havel, J. Silver or Silver Nanoparticles: A Hazardous Threat to the Environment and Human Health? *J. Appl. Biomed.* **2008**, *6* (3), 117–129. https://doi.org/10.32725/jab.2008.015.

(29) Quadros, M. E.; Marr, L. C. Environmental and Human Health Risks of Aerosolized Silver Nanoparticles. *J. Air Waste Manag. Assoc.* **2010**, *60* (7), 770–781. https://doi.org/10.3155/1047-3289.60.7.770.

(30) Yang, G.; Xie, J.; Hong, F.; Cao, Z.; Yang, X. Antimicrobial Activity of Silver Nanoparticle Impregnated Bacterial Cellulose Membrane: Effect of Fermentation Carbon Sources of Bacterial Cellulose. *Carbohydr. Polym.* **2012**, *87* (1), 839–845. https://doi.org/10.1016/j.carbpol.2011.08.079.

(31) Guzman, M.; Dille, J.; Godet, S. Synthesis and Antibacterial Activity of Silver Nanoparticles against Gram-Positive and Gram-Negative Bacteria. *Nanomedicine Nanotechnology, Biol. Med.* **2012**, *8* (1), 37–45. https://doi.org/10.1016/j.nano.2011.05.007.

(32) Tsuji, M.; Gomi, S.; Maeda, Y.; Matsunaga, M.; Hikino, S.; Uto, K.; Tsuji, T.; Kawazumi, H. Rapid Transformation from Spherical Nanoparticles, Nanorods, Cubes, or Bipyramids to Triangular Prisms of Silver with PVP, Citrate, and H 2O 2. *Langmuir* **2012**, *28* (24), 8845–8861. https://doi.org/10.1021/la3001027.

(33) Errokh, A.; Magnin, A.; Putaux, J. L.; Boufi, S. Hybrid Nanocellulose Decorated with Silver Nanoparticles as Reinforcing Filler with Antibacterial Properties. *Mater. Sci. Eng. C* **2019**, *105* (June). https://doi.org/10.1016/j.msec.2019.110044.

(34) Drogat, N.; Granet, R.; Sol, V.; Memmi, A.; Saad, N.; Klein Koerkamp, C.; Bressollier, P.; Krausz, P. Antimicrobial Silver Nanoparticles Generated on Cellulose Nanocrystals. *J. Nanoparticle Res.* **2011**, *13* (4), 1557–1562. https://doi.org/10.1007/s11051-010-9995-1.

(35) Jiang, F.; Hsieh, Y. Lo. Synthesis of Cellulose Nanofibril Bound Silver Nanoprism for Surface Enhanced Raman Scattering. *Biomacromolecules* **2014**, *15* (10), 3608–3616. https://doi.org/10.1021/bm5011799.

(36) Uddin, K. M. A.; Lokanathan, A. R.; Liljeström, A.; Chen, X.; Rojas, O. J.; Laine, J. Silver Nanoparticle Synthesis Mediated by Carboxylated Cellulose Nanocrystals. *Green Mater.* **2014**, *2* (4), 183–192. https://doi.org/10.1680/gmat.14.00010.

(37) Musino, D.; Devcic, J.; Lelong, C.; Luche, S.; Rivard, C.; Dalzon, B.; Landrot, G.; Rabilloud, T.; Capron, I. Impact of Physico-Chemical Properties of Cellulose Nanocrystal / Silver Nanoparticle Hybrid Suspensions on Their Biocidal and Toxicological Effects. *Submitted* **2020**.

(38) Reid, M. S.; Villalobos, M.; Cranston, E. D. Benchmarking Cellulose Nanocrystals: From the Laboratory to Industrial Production. *Langmuir* **2017**, *33* (7), 1583–1598. https://doi.org/10.1021/acs.langmuir.6b03765.

(39) Musino, D.; Rivard, C.; Landrot, G.; Novales, B.; Capron, I. Tunable Ag Nanoparticle Properties in Cellulose Nanocrystals/ Ag Nanoparticle Hybrid Suspensions by H2O2 Redox Post-Treatment: The Role Of The H2O2/Ag Ratio. *Nanomaterials* **2020**, *10(8)*, 1559.

(40) Khanjanzadeh, H.; Behrooz, R.; Bahramifar, N.; Gindl-Altmutter, W.; Bacher, M.; Edler, M.; Griesser, T. Surface Chemical Functionalization of Cellulose Nanocrystals by 3-Aminopropyltriethoxysilane. *Int. J. Biol. Macromol.* **2018**, *106*, 1288–1296. https://doi.org/10.1016/j.ijbiomac.2017.08.136.

(41) Rosset, A.; Bartolomei, V.; Laisney, J.; Shandilya, N.; Voisin, H.; Morin, J.; Michaud-Soret, I.; Capron, I.; Wortham, H.; Brochard, G.; Bergé, V.; Carriere, M.; Dussert, F.; Le Bihan, O.; Dutouquet, C.; Benayad, A.; Truffier-Boutry, D.; Clavaguera, S.; Artous, S. Towards the Development of Safer by Design TiO 2 -Based Photocatalytic Paint: Impacts and Performances . *Environ. Sci. Nano* **2021**, 758–772. https://doi.org/10.1039/d0en01232g.

(42) Musino, D.; Rivard, C.; Novales, B.; Landrot, G.; Rabilloud, T.; Capron, I. Hydroxyl Groups on Cellulose Nanocrystal Surfaces Form Nucleation Points for Silver Nanoparticles of Varying Shapes and Sizes (Accepted). *J. Colloid Interface Sci.* **2020**.

(43) Fiorentino, B.; Golanski, L.; Guiot, A.; Damlencourt, J. F.; Boutry, D. Influence of Paints Formulations on Nanoparticles Release during Their Life Cycle. *J. Nanoparticle Res.* **2015**, *17* (3). https://doi.org/10.1007/s11051-015-2962-0.

(44) Truffier-Boutry, D.; Fiorentino, B.; Bartolomei, V.; Soulas, R.; Sicardy, O.; Benayad, A.; Damlencourt, J. F.; Pépin-Donat, B.; Lombard, C.; Gandolfo, A.; Wortham, H.; Brochard, G.; Audemard, A.; Porcar, L.; Gebel, G.; Gligorovski, S. Characterization of Photocatalytic Paints: A Relationship between the Photocatalytic Properties-Release of Nanoparticles and Volatile Organic Compounds. *Environ. Sci. Nano* **2017**, *4* (10), 1998–2009. https://doi.org/10.1039/c7en00467b.

(45) Göhler, D.; Stintz, M.; Hillemann, L.; Vorbau, M. Characterization of Nanoparticle Release from Surface Coatings by the Simulation of a Sanding Process. *Ann. Occup. Hyg.* **2010**, *54* (6), 615–624. https://doi.org/10.1093/annhyg/meq053.

(46) Golanski, L.; Gaborieau, A.; Guiot, A.; Uzu, G.; Chatenet, J.; Tardif, F. Characterization of Abrasion-Induced Nanoparticle Release from Paints into Liquids and Air. *J. Phys. Conf. Ser.* **2011**, *304* (1). https://doi.org/10.1088/1742-6596/304/1/012062.

(47) Kisin, E. R.; Yanamala, N.; Rodin, D.; Menas, A.; Farcas, M.; Russo, M.; Guppi, S.; Khaliullin, T. O.; Iavicoli, I.; Harper, M.; Star, A.; Kagan, V. E.; Shvedova, A. A. Enhanced Morphological Transformation of Human Lung Epithelial Cells by Continuous Exposure to Cellulose Nanocrystals. *Chemosphere* **2020**, *250*, 126170. https://doi.org/10.1016/j.chemosphere.2020.126170.